Photonics-on-a-chip: recent advances in integrated waveguides as enabling detection elements for real-world, lab-on-a-chip biosensing applications

Adam L. Washburn and Ryan C. Bailey*

Received 27th June 2010, Accepted 10th September 2010
DOI: 10.1039/c0an00449a

By leveraging advances in semiconductor microfabrication technologies, chip-integrated optical biosensors are poised to make an impact as scalable and multiplexable bioanalytical measurement tools for lab-on-a-chip applications. In particular, waveguide-based optical sensing technology appears to be exceptionally amenable to chip integration and miniaturization, and, as a result, the recent literature is replete with examples of chip-integrated waveguide sensing platforms developed to address a wide range of contemporary analytical challenges. As an overview of the most recent advances within this dynamic field, this review highlights work from the last 2–3 years in the areas of grating-coupled, interferometric, photonic crystal, and microresonator waveguide sensors. With a focus towards device integration, particular emphasis is placed on demonstrations of biosensing using these technologies within microfluidically controlled environments. In addition, examples of multiplexed detection and sensing within complex matrices—important features for real-world applicability—are given special attention.

Introduction

By enabling efficient solution transport, mixing, separation, and analysis of small sample volumes on a single integrated fluidic chip, recent advances in microfluidic technologies have made possible the miniaturization and integration of many standard bioanalytical assays.[1] Although many lab-on-a-chip devices feature elegant fluid handling capabilities, the actual process of sample quantitation is often achieved with far less grace, requiring bulky and cumbersome instrumentation which, at some level, diminishes the overall utility of these miniature analytical devices. Of particular relevance are optical detection schemes that, while providing high sensitivity and assay versatility, can require large and expensive microscopy instrumentation.

Over the past several decades, fibre optic probes have been demonstrated as promising tools for chemical and biological sensing within small sample volumes.[2] However, these methods typically remain reliant upon external optical components and their sensitivity is often directly tied to the physical length of the fibre–sample interaction, meaning that ultrasensitive measurements

Department of Chemistry, Institute for Genomic Biology and Micro and Nanotechnology Laboratory, University of Illinois at Urbana-Champaign, 600 South Mathews Avenue, Urbana, Illinois, 61801, USA. E-mail: baileyrc@illinois.edu; Fax: +1 (217) 265-6290; Tel: +1 (217) 333-0676

Adam L. Washburn

Adam Washburn received a BS in Chemistry from Brigham Young University in 2006, and is currently a PhD candidate in the Department of Chemistry at the University of Illinois at Urbana-Champaign as a National Science Foundation Graduate Research Fellow working in the lab of Prof. Ryan Bailey. Adam's research is focused on the development of optical microring resonators for multiplexed proteomic applications.

Ryan C. Bailey

Ryan C. Bailey is an Assistant Professor in the Department of Chemistry at the University of Illinois at Urbana-Champaign and is affiliated with the University's Institute for Genomic Biology and Micro and Nanotechnology Laboratory. Ryan received his BS in Chemistry from Eastern Illinois University in 1999 and his PhD in Chemistry from Northwestern University in 2004, after which he was a joint postdoctoral fellow at the California Institute of Technology and Institute for Systems Biology. His research interests lie in the development of new multiparameter biological analysis technologies for applications in informative disease diagnostics, homeland security, and fundamental biological studies.

require larger probes that may no longer be amenable to small volume analyses.

Recent advances in microfabrication have enabled high density, chip-scale integration of optical components, such as light sources and photodetectors.[3–9] These devices offer substantial advantages for lab-on-a-chip applications by enabling integration of both fluidic handling and optical analysis onto a single chip. These types of integrated sensing devices have the potential to enable creation of high-density biosensors that can provide rapid, sensitive, and multiplexed measurements in point-of-care diagnostic applications.[10]

While significant advances have been made in the incorporation of light sources and detectors into chip-based analytical platforms, this review features another essential element of chip-integrated optical detection: waveguides. Propelled by advances in wafer-scale microfabrication over the past two decades, it is now relatively straightforward to incorporate many hundreds or even thousands of chip-integrated waveguides into a single sensor substrate, and this intrinsic scalability allows researchers to envision high levels of measurement multiplexing within small sample volumes.

Many examples, including several commercial products, exist in which integrated waveguides are used as excitation and/or collection elements for fluorescence-based sensors.[11,12] However, in this review, we primarily focus on chip-integrated biosensors that transduce the presence of a target analyte on the basis of binding-induced changes in the refractive index proximal to the waveguide surface. These devices are promising detection elements for a myriad of biosensing applications, largely due to the fact that they do not require the labelling of any biomolecule, a procedure that can perturb native interactions, as well as increase assay cost and complexity.[13] In particular, we will discuss advances within the past two to three years that have established grating-coupled, interferometric, photonic crystal, and microresonator-based waveguide sensors as promising biomolecular detection elements for lab-on-a-chip analytical applications.

The governing physics of waveguide operation and the concept of their utility as an analytical device are quite simple. Due to the contrast in refractive index between the core and cladding of an optical waveguide, light is guided through the device on account of total internal reflection, which generates an evanescent optical field that decays exponentially from the sensor surface. Biomolecular binding events modulate the refractive index contrast and thus attenuate the propagation of light through the waveguide. By monitoring the coupling and/or propagation properties of light through an appropriately modified waveguide, it is possible to construct sensors responsive to target biomolecular analytes of interest.

Although several outstanding reviews have addressed the pre-2008 state-of-the-art in waveguide sensing,[14–17] the last several years have been filled with tremendous advances that are reshaping the landscape of this rapidly evolving field. Furthermore, there exists a large body of literature discussing the fabrication, simulation, and preliminary evaluation of waveguide-based sensors; however, a far smaller number of reports describe actual experimental validation of these devices as microfluidically integrated detection elements. Thus, this review also serves to highlight the most recent progress in translating chip-integrated waveguides from cleanroom curiosities to relevant solutions for lab-on-a-chip biosensing applications, with special emphases given to papers that demonstrate sensing within complex matrices, as well as those papers that feature the ability to perform multiplexed detection using arrays of chip-integrated waveguide sensors.

Grating-coupled waveguide sensors

Grating-coupled waveguides are perhaps one of the most easily fabricated chip-integrated technologies for biosensing. A grating-coupled waveguide can be generated by creating a thin-film, single-mode, planar waveguide with a grating etched into an optical input region using photolithographic or imprinting techniques. Light is coupled into a waveguide mode if the following equation is satisfied:

$$n_{\mathrm{eff}} = n_{\mathrm{air}} \sin \alpha + l(\lambda/\Lambda),$$

where n_{eff} is the effective refractive index of the waveguide, n_{air} is the refractive index of air, α is the angle of incidence of the light, l is the diffraction order, λ is the wavelength of light, and Λ is the grating period.[18–20] Thus, a change in n_{eff} (*e.g.* from biomolecules binding to the waveguide surface) causes a change in the angle or wavelength at which light is maximally coupled into the waveguide.

Fig. 1 shows a schematic of a typical setup for the optical waveguide light-mode spectroscopy (OWLS) technique. As shown in the figure, light is coupled into the structure *via* the surface grating and the intensity propagating through the waveguide is measured by a photodetector near the output end of the waveguide. The angle of maximal coupling is determined by rotating the entire optical system relative to a fixed light source. Shifts in the angle of maximal coupling can then be correlated to changes in the refractive index within the evanescent sensing volume of the waveguide. When the waveguide is appropriately modified with biological recognition elements, OWLS can be used to monitor target analytes binding to the surface.

Several recent demonstrations of this technology for performing immunoassays on biomolecular targets have established

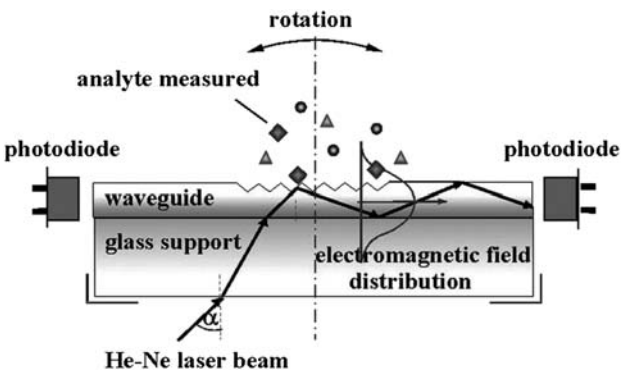

Fig. 1 Optical waveguide light-mode spectroscopy (OWLS) diagram as an illustration of the principle of grating-coupled waveguide biosensors. The angle of incidence at which light is maximally coupled into the waveguide varies with the effective refractive index of the waveguide. Figure adapted from ref. 19.

the potential for OWLS in biosensing. The commercialized OWLS platform (by MicroVacuum[17]) uses a single grating (2 × 12 mm) on a glass slide (8 × 12 mm) with a ~200 nm thick silicon/titanium oxide waveguide. Using this device and supporting instrumentation, Kim *et al.* have recently shown applicability to food safety monitoring by detecting flatfish vitellogenin[21] in purified fish serum samples as well as sulfamethazine in buffer.[22] Similarly, Adányi and co-workers have used OWLS to detect the mycotoxins, Aflatoxin B1 and Ochratoxin A, in the low ng mL^{-1} range in spiked wheat and barley samples using a competitive assay.[23] The same group also demonstrated the potential for measuring spiked concentrations of the herbicide trifluralin in apple juice, as well as the mycotoxin zearalenone in corn samples.[19]

In addition to determining concentrations of biomolecules in solution, OWLS has also been used to study the adsorption and conformation of biomolecules on a surface.[24–26] For example, Zhang *et al.* measured the binding kinetics of vascular endothelial growth factor (VEGF) binding to surface immobilized extracellular domain 3 of the human VEGF Receptor-2 (VEGFR-2).[27] OWLS sensors have also been used extensively for monitoring the binding of bacteria, such as *Legionella pneumophila*[28] and *Salmonella typhimurium*,[29] to the sensor surface.

One of the unique advantages demonstrated by OWLS (as compared to other waveguide sensors) is the ability to fabricate the dielectric waveguide from transparent and electroactive materials. For example, Adányi *et al.* used a sensor chip coated with conductive indium tin oxide to apply a potential to the surface, which created a charge polarization that facilitated electrostatic adsorption of bacteria on the surface.[30] Eggleston *et al.* coated the waveguide sensor with Al_2O_3 and Fe_2O_3 in order to observe differential adsorption of outer-membrane c-type cytochrome (OmcA) onto a model biofuel cell electrode.[31]

Although the OWLS system has been widely used for many types of bioassays, one significant drawback at present is that there is typically only a single grating-coupled waveguide sensor per chip. This single sensor format not only prohibits the simultaneous assaying of multiple target analytes, but also signifies an inability to include on-chip controls and references for changes in bulk solution (not surface-specific) refractive index as well as thermally based refractive index drift. Furthermore, this greatly complicates detection within complex samples since it can be nearly impossible to separate specific and non-specific surface binding events.

Another grating-based waveguide technique featuring a much higher number of sensors per chip is wavelength-interrogated optical sensors (WIOS). Similar to OWLS, WIOS uses gratings to couple light into the waveguide, but rather than measuring the coupling efficiency as a function of angle, the coupling is measured as a function of wavelength. In addition, light is out coupled from the chip *via* a grating (called the output pad) which has a different period than the input pad and directs light to an unattached photodetector, as shown in Fig. 2A. The difference in grating period between the input and output pads prevents interference between the in- and out-coupled light.[32] Using these sensors, a mass sensitivity of 0.3 pg mm^{-2} has been reported.[20] The ability to incorporate multiple sensors onto a single substrate (as shown in Fig. 2B) makes WIOS amenable to multiplexed measurements, as well as on-chip referencing.

Adrian and co-workers applied WIOS in a competitive immunoassay to analyze antibiotic residues in milk.[33] By using a WIOS chip integrated within a fluidic cartridge, they were able to measure sulfonamide antibiotic residues at levels down to 0.5 μg L^{-1}. After demonstrating the ability to perform single parameter assays, the same group then utilized the multiplexing capabilities of their sensors to detect multiple antibiotic residues on a single chip.[34,35] Using the WIOS chip, they were able to measure fluoroquinolone, sulfonamide, β-lactam, and tetracycline residues and determine whether their concentrations exceeded the 100 μg mL^{-1} safety threshold with 95% accuracy in

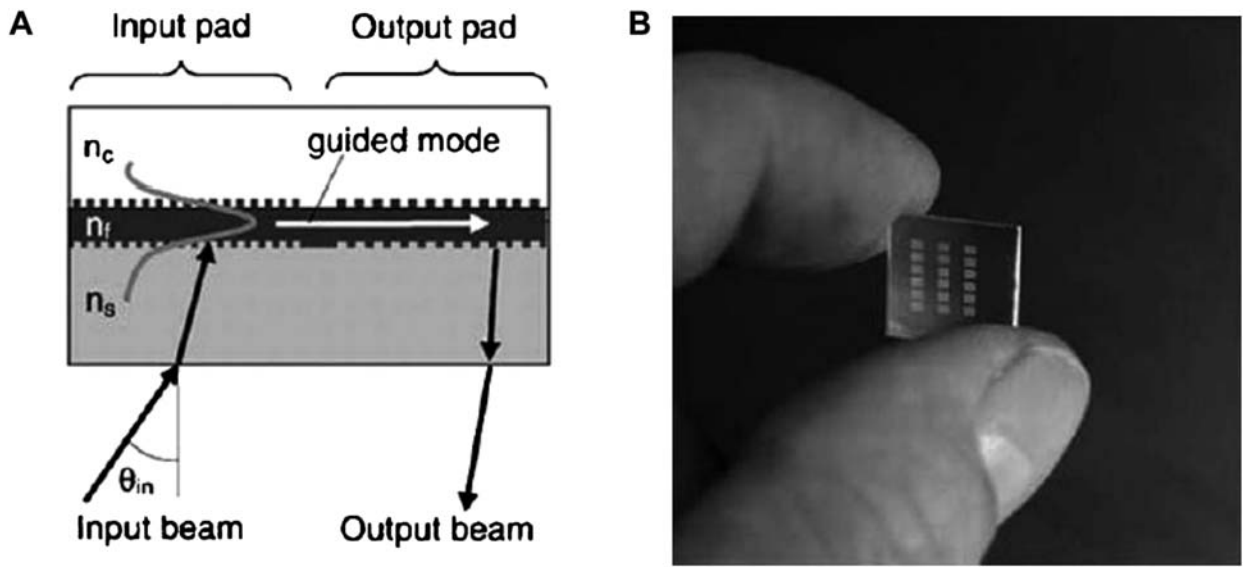

Fig. 2 (A) Scheme for wavelength-interrogated optical sensor (WIOS) with input and output grating couplers. The wavelength required to maximally couple light into the waveguide changes as the refractive index above the waveguide changes. (B) A picture showing multiple sensors on a single chip. Figure adapted from ref. 32.

6 blind unknown milk samples. Thus, with improved sensitivity and multiplexing capabilities, the WIOS system shows tremendous promise for looking at real-world samples in a lab-on-a-chip setting, with several key advantages over the simpler OWLS setup.

Interferometric waveguide sensors

Waveguide sensors that involve an interferometric method for measuring changes in refractive index provide another chip-based method for detecting biomolecular binding. One of the most common formats for on-chip interferometric sensing is an integrated Mach–Zehnder interferometer (MZI). Fig. 3A illustrates the general principle of a standard free space MZI. Initially, light is divided at a beam splitter into two paths with one light path containing a sample and the other path acting as a reference. The higher refractive index of the sample changes the phase of light in that path so that constructive or destructive interference occurs upon beam recombination at the second beam splitter. This in turn modulates the light intensity at the photodetector, which then can be used to determine the difference in refractive index between the sample and the reference.

As shown in Fig. 3B, a chip-based MZI follows the same principle as a free space MZI except that light is coupled down a waveguide and is split into two parallel paths at a Y-junction and then recombined after a fixed distance.[36] Biomolecular binding occurs on the sensing arm, and by monitoring the phase shift of light hitting the photodetector, it is possible to sensitively monitor the change of refractive index near the surface of the sensing arm waveguide. Additionally, because the sample and reference arms are in close proximity, any effects of thermal drift typically cancel out resulting in a fairly temperature insensitive measurement.

Chip-based MZIs exhibit a high sensitivity to local changes in refractive index and have been demonstrated to show refractive index sensitivity down to 10^{-6} to 10^{-7} refractive index units (RIUs).[37–40] When the surface of the sensing arm is modified so as to present an appropriate recognition element, this index sensitivity can be used to achieve limits of detection of 1 pg mm^{-2} for bound mass at the surface, similar to the limit of detection for grating-coupled waveguide sensors.[37]

The versatility of the MZI sensor design makes it amenable to a variety of material systems, with recent reports of devices fabricated from silicon oxides,[41–43] silicon nitride,[36] or silicon-on-insulator (SOI),[44] and even polymers.[45,46] Another interesting MZI configuration involves use of liquid core waveguides for the sensing arm, wherein the fluidic delivery system is actually within the optical sensor itself.[39,47] Some variations in MZI design in the recent literature include work by Kitsara *et al.* using a white light source and spectrophotometer,[48] thus eliminating the need for a laser source, and Kim *et al.*, who introduced a power splitting junction before the standard MZI junction to account for variations in optical power.[49]

As another variation in MZI design, Crespi *et al.* have shown that 3-D Mach–Zehnder structures can be incorporated into microfluidic devices using ultrafast laser writing.[42] By utilizing the laser writing technique, 3-D waveguides are fabricated in a fused silica substrate perpendicular to a conventional microfluidic channel on the same substrate. The sensing arm of the MZI is designed to pass in proximity to the microfluidic channel, whereas the reference arm passes around the microfluidic channel. As a result, any changes in refractive index within the microfluidic channel can be measured *via* the MZI. Because the MZIs are perpendicular to the microfluidic channel, multiple MZIs can be fabricated along the length of the channel enabling the measurement of changes in refractive index at several points along the microfluidic channel. This is an advantage for applications such as capillary electrophoresis because the multiple MZI sensors provide both spatial and temporal information regarding changes in refractive index during the course of a separation. Using such a device, the authors were able to show detection of mM concentrations of peptides in solution.

For planar, chip-integrated MZIs, several groups have recently shown the applicability of these devices to bioanalytical challenges of contemporary importance. Xu and coworkers have demonstrated the ability to detect avian influenza virus H7 on an MZI chip in both direct and sandwich immunoassay formats down to a concentration of 0.0005 hemagglutination units per

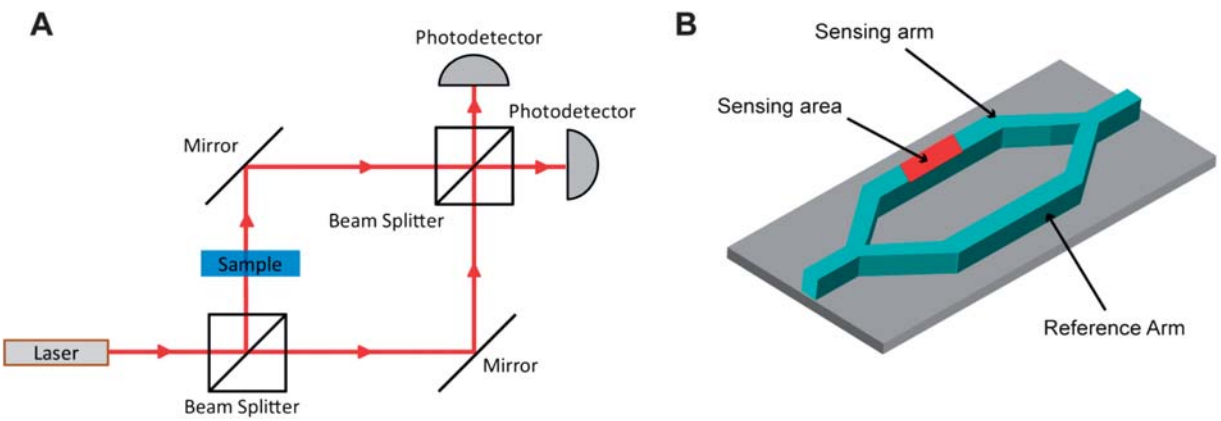

Fig. 3 (A) A schematic of a classic free space Mach–Zehnder interferometer. Light from a light source is split into two paths (sample and reference) at a beam splitter and then recombined at another beam splitter whereupon the degree of interference is measured at a photodetector. The interference is due to a higher refractive index sample slowing down the light in the sample path. (B) Illustration of an on-chip Mach–Zehnder interferometer with a Y-junction splitting a waveguide into a sensing arm and a reference arm.

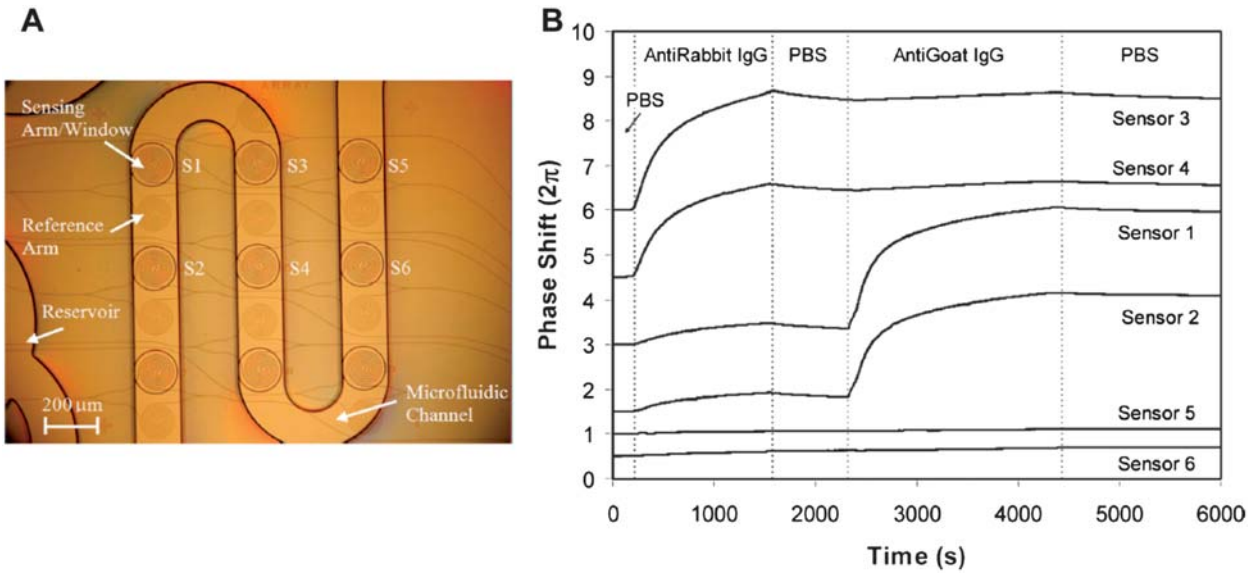

Fig. 4 (A) Picture showing the layout of six MZI sensors on a chip in an integrated microfluidic channel. (B) Real time biosensing data showing specific sensor response to Anti-rabbit IgG (sensors 3 and 4) and anti-goat IgG (sensors 1 and 2) with sensors 5 and 6 as controls. Figure adapted from ref. 50.

mL in buffer.[40] Shew and coworkers demonstrated the detection of IgG down to 1 ng mL^{-1} using a direct binding assay in buffer.[45] They also incorporated a horseradish peroxidase amplification step to catalyze tetramethylbenzidine conversion resulting in a change in the solution refractive index. This lowered the limit of detection down to 1 pg mL^{-1} in buffer for a one-hour incubation period.

For nucleic acid analysis, the Lechuga group has shown label-free detection of DNA in buffer using a chip-integrated MZI.[37] Using the same capture probe, they were able to measure binding of both a wild type sequence (58-mer) and mutated sequence from 10 pM to 1 μM. Although both sequences bound to their capture probe, they were able to show that the binding occurred with differing affinities.

Although many of these devices have shown promise for the detection of biological molecules, most of the systems have single MZI designs, limiting the ability to multiplex or include control measurements (*i.e.* another MZI reference/sensing arm pair without a capture agent on the sensing arm). By contrast, Densmore *et al.* recently demonstrated the incorporation of multiple sensors onto a single chip using a spiral arm MZI design on a SOI substrate.[50] Each of these sensors can be uniquely functionalized *via* microspotting and the entire array can be incorporated within a microfluidic device, as shown in Fig. 4A. Importantly, the spiral design of these sensors increases the effective path length of the sensing arm, boosting the device sensitivity towards biomolecular binding. Using these arrays, they have demonstrated the ability to simultaneously monitor six different sensors and show that each responds specifically to different antigens, as dictated by the capture agent attached to each MZI.

Fig. 4B shows three sets of sensors (two in each set for a total of six), with each set functionalized with a different capture agent. Sensors 3 and 4 are functionalized with rabbit IgG, sensors 1 and 2 are functionalized with goat IgG, and sensors 5 and 6 are not functionalized but rather serve as negative controls. As a result, after a solution containing anti-rabbit IgG is introduced, sensors 3 and 4 respond but no response is seen from the other 4 sensors. Similarly, upon introduction of anti-goat IgG, sensors 1 and 2 respond, but the other 4 show no significant response. While this report does not push the ultimate sensitivity of the device, it clearly demonstrates the feasibility of multiplexed biosensing using chip-integrated MZIs.

Although all of the MZI sensors have shown the ability to sensitively measure biomolecules in a label-free manner, many of these demonstrations have focused on simple systems consisting of a single analyte in buffer. Examples of detection from within more complex samples appear to be the next step for these devices as they strive for real-world applicability.

In addition to the Mach–Zehnder-style interferometer, chip-integrated Young interferometers have also shown promise for biosensing. Like the MZI, the Young interferometer has multiple Y-junctions for splitting light into two separate paths with one

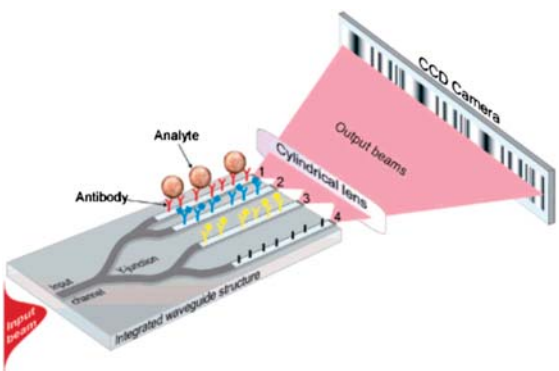

Fig. 5 Diagram showing the principle of a Young interferometer. Rather than rejoining the waveguides after the Y-junction, the light is projected onto a CCD camera giving an interference pattern. Figure adapted from ref. 50.

arm as a sensing arm and one arm as a reference arm, as shown in Fig. 5. However, rather than rejoining the two arms and measuring the interference of the light based on the intensity of the recombined light, the light is projected off chip and onto a CCD camera, where the interference pattern is imaged. By monitoring changes in the interference fringes with the CCD camera, it is possible to sensitively measure phase changes of light in the sensing arms and thus infer changes in refractive index.

Using such a technique, Hoffman and co-workers have demonstrated the detection of IgG,[51] and Schmitt *et al.* reported on the sensing of a proprietary binding tag[52] on a protein with a sub-nanomolar limit of detection and with an estimated sensitivity of bound surface mass of 13 fg mm^{-2}—an unmatched bound surface mass sensitivity compared to the other techniques reviewed in this paper. Similarly, Ymeti *et al.* have demonstrated the detection of human serum albumin as well as HSV-1 virus particles down to 10^5 particles per mL.[53] Unfortunately, despite these intriguing early examples, dating from 2007, there appears to have been very little subsequent work directed towards developing Young interferometers as sensitive biosensors.

Photonic crystal waveguide sensors

Photonic crystal waveguides comprise another system that is promising for chip-integrated refractive index based sensing. Photonic crystal waveguides consist of periodic arrays of dielectric structures optically connected to a standard planar waveguide. By introducing defects into the periodic structure of the photonic crystal region, certain frequencies of light become resonantly confined within the defect structures resulting in a high localized optical field density near the defect.[54] The exact frequency of light that is coupled into the photonic crystal is a function of the refractive index in the volume immediately surrounding the defect, and thus molecular binding to the photonic crystal substrate induces a change in the resonance frequency of the device.

Although a TiO_2-coated polymer has been very successfully used for microplate-based photonic crystal biosensors,[55] SOI appears to be the substrate of choice for chip-integrated photonic crystals.[56] Typically, electron beam lithography is used to fabricate arrays of holes with carefully positioned defects adjacent to a planar silicon waveguide on a SOI substrate.[57–61] Fig. 6A shows an SEM image of a photonic crystal waveguide on a SOI surface.

The Fauchet group has utilized such a system for detecting proteins in solution. For example they have demonstrated the ability to measure μg mL^{-1} concentrations of human IgG with anti-human IgG capture agents,[54] as well as the non-specific interactions of BSA binding to their surface *via* glutaraldehyde mediated cross-linking.[57] Similarly Zlatanovic and coworkers have shown that they can detect anti-biotin antibodies binding to biotinylated BSA on their photonic crystal surface allowing determination of the capture agent binding affinity.[58] Dorfner *et al.*[60] and Skivesen *et al.*[61] have shown that they can detect physisorbed BSA, and Buswell *et al.* have shown that they can detect streptavidin binding to a biotin-functionalized surface.[59] Although many of these reports do not demonstrate extremely low limits of detection in terms of analyte concentration, the small size of the sensing area (~50 $μm^2$) means that they are sensitive down to femtogram quantities of bound protein on the surface.[57,58,60]

As a variation on the 2-D photonic crystal waveguides used by the previous groups, Mandal and Erickson have developed a chip-integrated microresonator system with multiple waveguides attached to an array of 1-D photonic crystal resonators etched out of silicon on a SOI substrate.[62] Not only have they demonstrated that they can create such a system with 16 integrated sensors on a single chip, as shown in Fig. 6B, but they have utilized their system for the multiplex detection of three different cytokines (interleukins 4, 6, and 8) using a sandwich assay detection format.[63] This report confirmed the potential for photonic crystal waveguide sensors to sensitively detect multiple analytes simultaneously.

Most reports of chip-integrated photonic crystal biosensors have focused on relatively simple systems and proof-of-principle assays and, like most of the techniques featured in this review, need to demonstrate their applicability to real-world samples. Furthermore, the literature indicates that most photonic crystal waveguide sensors have much lower (worse) sensitivity in terms of mass per unit area when compared to the other sensors highlighted in this review. However, the extremely small sensing area suggests that these sensors could be very well suited to applications faced with extremely limited sample volumes.

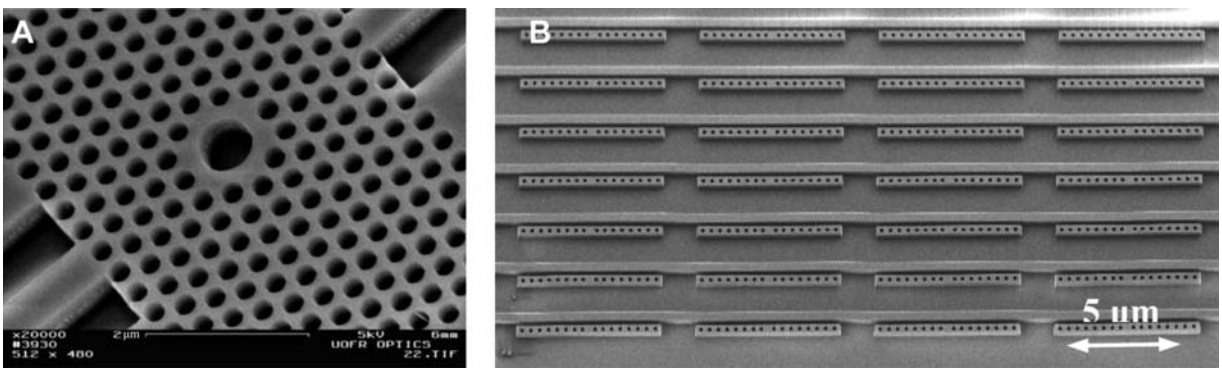

Fig. 6 (A) SEM image showing a photonic crystal waveguide made of an array of nanometre-scale holes in a SOI substrate. The large hole in the centre is the defect where electric field is focused and where the device is most sensitive to changes in refractive index. Figure adapted from ref. 56. (B) SEM image of arrays of 1-D photonic crystal resonators adjacent to linear waveguides. Figure adapted from ref. 62.

Resonant optical microcavity sensors

Another class of waveguide devices that have been investigated as chip-integrated biosensors are resonant optical microcavities.[17] These sensors, which can be fabricated out of a variety of materials and with several similar, but distinct, cavity geometries, generally function by coupling light from an adjacent linear waveguide into a circular microcavity. Optical interference between photons in the linear waveguide and microcavity dictates that only specific wavelengths of light are resonantly supported, as defined by the equation:

$$m\lambda = 2\pi r n_{\text{eff}}$$

where m is an integer, λ is the wavelength of light, r is the radius of the ring, and n_{eff} is the effective refractive index of the waveguide mode.

When fabricated with very high precision and limited cavity surface roughness, the resonance peaks become incredibly spectrally narrow and the structures are referred to as high Q (quality) factor cavities. The narrow peaks facilitate resolution of small shifts in the spectral position of the resonance, making these devices very sensitive to the local refractive index near the resonator. By functionalizing the microcavities with appropriate biomolecular capture agents, binding induced changes in refractive index are transduced *via* a shift in the optical wavelengths resonantly supported by the structure. This concept is schematically illustrated for the case of a microring resonator in Fig. 7A wherein biomolecular (protein) binding to a capture agent modified cavity (shown functionalized with antibody) causes the resonance wavelength to shift (black trace to red trace).

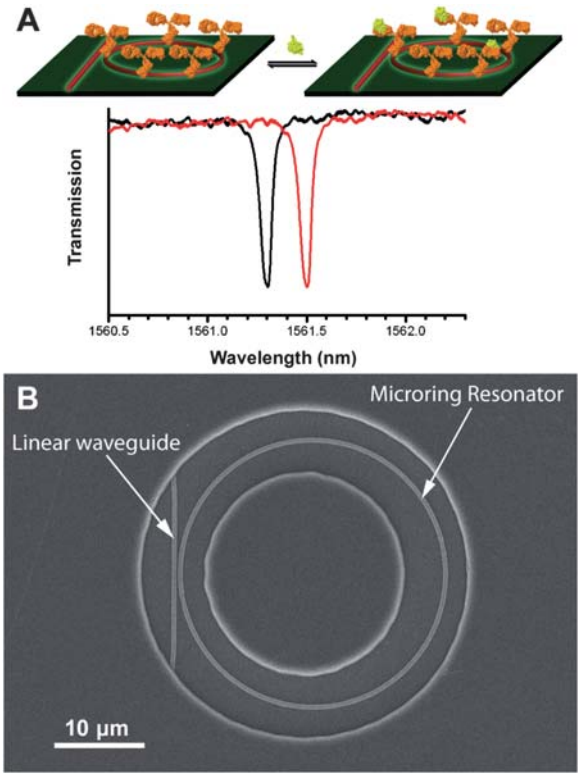

Fig. 7 (A) Illustration of proteins binding to a microring resonator and the subsequent shift of the resonance frequency. (B) SEM image of a SOI microring resonator as revealed through an annular opening in a polymeric cladding layer that confines solution flow and biological binding events to the area immediately surrounding the microring. Figure adapted from ref. 73.

Microsphere,[64] microtoroid,[65] and microcapillary[66] cavities have been reported to have tremendous detection sensitivities, occasionally down to the level of resolving single binding events. However, these devices are not readily fabricated in a chip-based format and optical interrogation of such cavities is not trivial (often requiring positioning of extruded optical fibres with nanometre precision and alignment). For this reason, microring resonators with chip-integrated linear access waveguides have emerged as promising candidates for scalable and multiplexable biosensing. Although the Q factor is lower for planar microcavity formats, as opposed to sphere, microtoroid, or capillary designs, the robust nature of the device in terms of ease in sensor interrogation, fabrication scalability, and functionalization offers advantages for applications in multiplexed biomolecular detection.

Similar to chip-based MZI sensors, microring resonator sensors can be fabricated from a variety of materials, including polymers,[67] silicon oxide,[68,69] silicon nitride,[70,71] and SOI.[72–74] Fig. 7B shows a scanning electron micrograph of a single microring resonator with corresponding linear access waveguide fabricated in the top layer of SOI. Typical sensitivities enable discrimination of changes in refractive index of 10^{-6} or better.[71,75–77] In their most basic format, these sensors feature a single microring coupled horizontally to a linear waveguide, but methods have been devised for vertical coupling.[76] Furthermore, coiled[78] and slotted[70,79] microring waveguides have also been demonstrated as well as Mach–Zehnder-integrated microrings, which show promise for increased sensitivity but at present face a potential drawback of reduced thermal stability.[80,81]

Because the microring resonator format is readily amenable to highly scalable and commercially validated microfabrication approaches, several groups have demonstrated the ability to fabricate arrays of microring resonators on a single chip. These sensors have been used for quantitative analysis of biological samples as well as multiplexed sensing. For example, Ramachandran *et al.* have demonstrated a chip with five microring sensors and have shown that they could derivatize the rings with antibodies against *Escherichia coli*.[69] These functionalized rings respond specifically to *E. coli* in comparison to unresponsive control rings. In the same paper the authors also showed specific binding of nucleic acids, as well as quantifying IgG binding. Subsequently, Wang and co-workers used an identical microring resonator array to monitor physical changes in cell behaviour upon exposure to cytotoxic chemicals.[82]

Carlborg and co-workers have demonstrated the utility of slotted microring resonators by developing a chip that contains 8 integrated microring resonators, 6 of which can be used as active sensing rings and 2 of which are employed as thermal controls.[71] Furthermore, this sensor chip was incorporated into a microfluidic casing that enabled independent fluidic access to each microring, which was then used to monitor the attachment of anti-BSA antibodies to the microcavities with good sensitivity.

Our group has also recently reported a chip-integrated SOI microring resonator array architecture consisting of 32 microrings on a single sensing substrate, allowing 24 microrings to be used as active biosensors with the other 8 functioning as thermal controls. With a sensitivity down to 1.5 pg mm^{-2} bound surface mass,[83] which is comparable to many of the other chip-integrated techniques described in this paper, we have shown the ability to detect the cancer biomarker carcinoembryonic antigen (CEA) at clinically relevant levels in both buffer and undiluted foetal bovine serum.[73] We have also demonstrated the monitoring of interleukin-2 (IL-2) secretion from stimulated Jurkat T-cells in cell-free culture media using a sandwich assay approach.[84] Changes in secreted IL-2 levels were monitored over a period of 24 hours post-stimulation, and the results were found to be in excellent correlation with a commercial ELISA assay, with an added advantage of enhanced measurement precision.

Focusing on applications in multiplexed biosensing, we have also created a sensor chip capable of simultaneously assaying for five different disease biomarkers.[85] By using a six-channel microfluidic device, we uniquely functionalized groups of four microrings with five different protein-specific antibodies and reserved one final group of four microrings as thermal and non-specific binding controls. Following functionalization, a single channel microfluidic gasket was placed over the chip enabling mixtures of antigen solutions to flow over all of the rings simultaneously. Fig. 8A shows the resulting concentration-dependent shifts in resonance wavelength for each of the 20 label-free immunoassays. Using this sensor array we demonstrated the ability to accurately determine the concentration of five different antigens in three different unknown cocktail solutions.

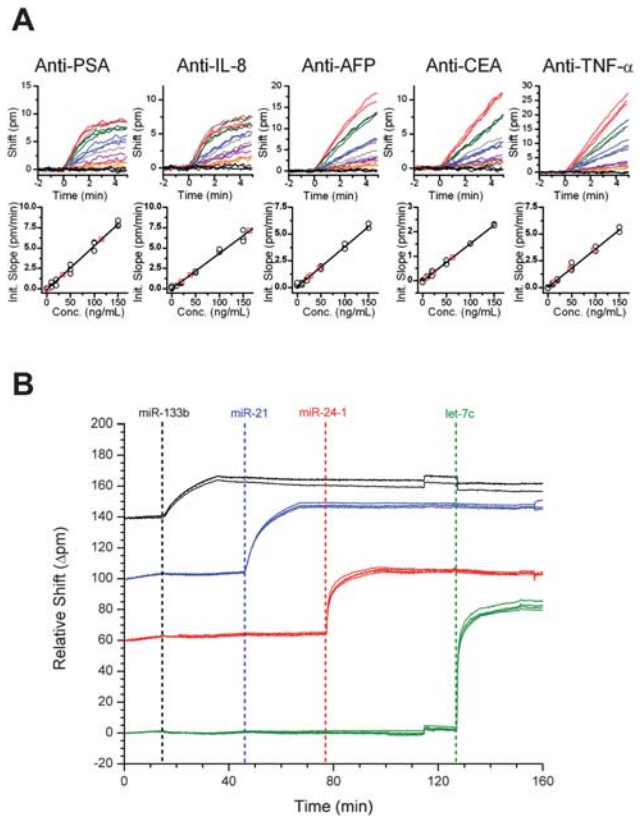

Fig. 8 (A) Real-time detection plots for 5 different microrings, each functionalized with a different antigen. The different colours indicate the different concentrations (10–150 ng mL^{-1}) of the particular antigen with the gray traces representing the unknowns being measured. Below each plot is the calibration curve generated from the data. Figure adapted from ref. 85. (B) Specific detection of four different miRNAs on a multiplexed chip. Each colour represents a different set of rings functionalized with a different set of DNA capture probes specific to each miRNA type. Figure adapted from ref. 86.

In addition to proteins, we also recently demonstrated the ability to detect microRNAs (miRNAs) using an array of chip-integrated microring resonators.[86] Using a direct hybridization assay with DNA capture probes, we demonstrated the ability to detect four different miRNAs on a single sensor chip, as shown in Fig. 8B. We determined the limit of detection for this first generation experiment to be 150 fmol after only a 10 minute assay and also showed the ability to discriminate between strands differing in sequence by only a single base. We then applied this platform to quantify the same four miRNAs isolated from a cell line model of glioblastoma.

Although initial results have shown promise for multiplexed detection and sensing in complex samples, non-specific binding still poses a major challenge to performing multiplexed biomolecular quantitation in relevant sample matrices. Detection can be achieved, but the limits of detection are typically worse when the sensor is operated in a more complex medium such as blood serum or tissue lysate. Also, many samples of interest require sensitivities in ranges below what the microrings can accurately measure at present. Therefore, approaches for improving device sensitivity and improving the underlying surface chemistry to promote specific, as opposed to non-specific, analyte binding remain areas of intensive research.

Together, we feel that the collective efforts of several groups have established microring resonators as promising candidates for chip-integrated biomolecular detection, and in particular multiplexed, label-free analysis. In addition, the demonstrated analytical capability of microring resonators to operate in complex samples highlights the significant potential for this class of detection elements to transition from a proof-of-concept technology to useful laboratory tool.

Conclusion

On account of scalable fabrication and relevant sensitivities for biomolecular sensing, chip-integrated waveguide structures are promising detection elements for many lab-on-a-chip applications. A variety of waveguide geometries and operational principles are currently under investigation and most feature an intrinsic multiplexing capability, a free benefit of using well-established microfabrication technologies.

In terms of sensitivity, grating-coupled, interferometric, and resonant microcavity sensors have comparable sensitivities (~1 pg mm^{-2}), which are generally an order of magnitude better than literature reports of photonic crystal based sensors. Although each of these sensor classes has been utilized in a multiplexed format, many still have yet to move beyond proof-of-principle demonstrations. Furthermore, the combination of multiplexed sensing from within biologically complex samples has yet to be fully achieved using any type of chip-integrated waveguide sensor.

Over the coming years, the keys to translating these sensors from academic novelties to viable laboratory tools lie in the design of robust sensor architectures and interrogation instrumentation that facilitate the integration of cutting edge optics into easily used lab-on-a-chip formats. Moreover, in order for waveguide based sensors to realize their full potential, researchers will also have to draw upon diverse expertises that extend beyond optics, as concerns such as surface chemistry, fluid dynamics, and biological assay design will increasingly dictate the overall performance of advanced sensor systems. Although much remains to be done, the future certainly appears bright for chip-integrated waveguide biosensors and the extension of these devices towards real-world biosensing applications should yield exciting results and enabling platforms for emerging bioanalytical challenges.

Acknowledgements

We acknowledge support for own efforts to develop chip-integrated waveguide biosensors from the NIH Director's New Innovator Award Program, part of the NIH Roadmap for Medical Research, through grant number 1-DP2-OD002190-01, and from the Camille and Henry Dreyfus Foundation. A.L.W. was supported *via* a National Science Foundation Graduate Research Fellowship.

References

1 S. Haeberle and R. Zengerle, *Lab Chip*, 2007, **7**, 1094–1110.
2 O. S. Wolfbeis, *Anal. Chem.*, 2008, **80**, 4269–4283.
3 N. M. Jokerst, L. Luan, S. Palit, M. Royal, S. Dhar, M. A. Brooke and T. Tyler, *IEEE Trans. Biomed. Circuits Syst.*, 2009, **3**, 202–211.
4 C. Monat, P. Domachuk and B. J. Eggleton, *Nat. Photonics*, 2007, **1**, 106–114.
5 L. Lin, R. D. Evans, N. M. Jokerst and R. B. Fair, *IEEE Sens. J.*, 2008, **8**, 628–635.
6 A. Banerjee, Y. Shuai, R. Dixit, I. Papautsky and D. Klotzkin, *J. Lumin.*, 2010, **130**, 1095–1100.
7 S. Vengasandra, Y. Cai, D. Grewell, J. Shinar and R. Shinar, *Lab Chip*, 2010, **10**, 1051–1056.
8 X. Wang, O. Hofmann, R. Das, E. M. Barrett, A. J. deMello, J. C. deMello and D. D. C. Bradley, *Lab Chip*, 2007, **7**, 58–63.
9 J. R. Wojciechowski, L. C. Shriver-Lake, M. Y. Yamaguchi, E. Füreder, R. Pieler, M. Schamesberger, C. Winder, H. J. Prall, M. Sonnleitner and F. S. Ligler, *Anal. Chem.*, 2009, **81**, 3455–3461.
10 F. S. Ligler, *Anal. Chem.*, 2008, **81**, 519–526.
11 H. Mukundan, A. S. Anderson, W. K. Grace, K. M. Grace, N. Hartman, J. S. Martinez and B. I. Swanson, *Sensors*, 2009, **9**, 5783–5809.
12 C. R. Taitt, G. P. Anderson and F. S. Ligler, *Biosens. Bioelectron.*, 2005, **20**, 2470–2487.
13 A. J. Qavi, A. L. Washburn, J. Y. Byeon and R. C. Bailey, *Anal. Bioanal. Chem.*, 2009, **394**, 121–135.
14 D. Psaltis, S. R. Quake and C. Yang, *Nature*, 2006, **442**, 381–386.
15 X. Fan, I. M. White, S. I. Shopoua, H. Zhu, J. D. Suter and Y. Sun, *Anal. Chim. Acta*, 2008, **620**, 8–26.
16 D. Erickson, S. Mandal, A. H. J. Yang and B. Cordovez, *Microfluid. Nanofluid.*, 2008, **4**, 33–52.
17 F. Vollmer and S. Arnold, *Nat. Methods*, 2008, **5**, 591–596.
18 K. Tiefenthaler and W. Lukosz, *J. Opt. Soc. Am. B*, 1989, **6**, 209–220.
19 A. Székács, N. Adányi, I. Székács, K. Majer-Baranyi and I. Szendrő, *Appl. Opt.*, 2009, **48**, B151–B158.
20 K. Cottier, M. Wiki, G. Voirin, H. Gao and R. E. Kunz, *Sens. Actuators, B*, 2003, **91**, 241–251.
21 N. Kim, H.-S. Ryu and W.-Y. Kim, *J. Microbiol. Biotechnol.*, 2007, **17**, 1445–1451.
22 N. Kim, D.-K. Kim and W.-Y. Kim, *Food Chem.*, 2008, **108**, 768–773.
23 N. Adányi, I. A. Levkovets, S. Rodriguez-Gil, A. Ronald, M. Váradi and I. Szendrő, *Biosens. Bioelectron.*, 2007, **22**, 797–802.
24 R. Horvath, J. McColl, G. E. Yakubov and J. J. Ramsden, *J. Chem. Phys.*, 2008, **129**, 071102.
25 M. Kroslak, J. Sefcik and M. Morbidelli, *Biomacromolecules*, 2007, **8**, 963–970.
26 S. Kurunczi, R. Horvath, Y.-P. Yeh, A. Muskotál, A. Sebestyén, F. Vonderviszt and J. J. Ramsden, *J. Chem. Phys.*, 2009, **130**, 011101.
27 J. Zhang, H. Li, W. Chen, P. Cao and M. Wang, *Biotechnol. Prog.*, 2009, **25**, 1703–1708.
28 I. R. Cooper, S. T. Meikle, G. Standen, G. W. Hanlon and M. Santin, *J. Microbiol. Methods*, 2009, **78**, 40–44.
29 N. Kim, I.-S. Park and W.-Y. Kim, *Sens. Actuators, B*, 2007, **121**, 606–615.
30 E. Németh, N. Adányi, A. Halász, M. Váradi and I. Szendro, *Biomol. Eng.*, 2007, **24**, 631–637.
31 C. M. Eggleston, J. Vörös, L. Shi, B. H. Lower, T. C. Droubay and P. J. S. Colberg, *Inorg. Chim. Acta*, 2008, **361**, 769–777.
32 A. M. Popa, B. Wenger, E. Scolan, G. Voirin, H. Heinzelmann and R. Pugin, *Appl. Surf. Sci.*, 2009, **256S**, S12–S17.
33 J. Adrian, S. Pasche, J.-M. Diserens, F. Sánchez-Baeza, H. Gao, M. P. Marco and G. Voirin, *Biosens. Bioelectron.*, 2009, **24**, 3340–3346.
34 G. Suárez, Y. H. Jin, J. Auerswald, S. Berchtold, H. F. Knapp, J. M. Diserens, Y. Leterrier, J. A. E. Månson and G. Voirin, *Lab Chip*, 2009, **9**, 1625–1630.
35 J. Adrian, S. Pasche, D. G. Pinacho, H. Font, J.-M. Diserens, F. Sánchez-Baeza, B. Granier, G. Voirin and M.-P. Marco, *TrAC, Trends Anal. Chem.*, 2009, **28**, 769–777.
36 B. Sepúlveda, J. S. del Río, M. Moreno, F. J. Blanco, K. Mayora, C. Domínguez and L. M. Lechuga, *J. Opt. A: Pure Appl. Opt.*, 2006, **8**, S561–S566.
37 J. S. del Río, L. G. Carrascosa, F. J. Blanco, M. Moreno, J. Berganzo, A. Calle, C. Domínguez and L. M. Lechuga, *Silicon Photonics II*, SPIE, San Jose, CA, USA, 2007.
38 R. G. Heideman and P. V. Lambeck, *Sens. Actuators, B*, 1999, **61**, 100–127.
39 P. Dumais, C. L. Callender, J. P. Noad and C. J. Ledderhof, *Opt. Express*, 2008, **16**, 18164–18172.
40 J. Xu, D. Suarez and D. Gottfried, *Anal. Bioanal. Chem.*, 2007, **389**, 1193–1199.
41 C. Themistos, M. Rajarajan, B. M. A. Rahman and K. T. V. Grattan, *J. Lightwave Technol.*, 2009, **27**, 5537–5542.
42 A. Crespi, Y. Gu, B. Ngamsom, H. J. W. M. Hoekstra, C. Dongre, M. Pollnau, R. Ramponi, H. H. van den Vlekkert, P. Watts, G. Cerullo and R. Osellame, *Lab Chip*, 2010, **10**, 1167–1173.
43 J. Hong, J. S. Choi, G. Han, J. K. Kang, C.-M. Kim, T. S. Kim and D. S. Yoon, *Anal. Chim. Acta*, 2006, **573–574**, 97–103.
44 A. Densmore, D.-X. Xu, P. Waldron, S. Janz, A. Delage, P. Cheben and J. Lapointe, *Silicon Photonics II*, SPIE, San Jose, CA, USA, 2007.
45 B. Y. Shew, Y. C. Cheng and Y. H. Tsai, *Sens. Actuators, A*, 2008, **141**, 299–306.
46 R. Bruck and R. Hainberger, *Photonics, Devices, and Systems IV*, SPIE, Prague, Czech Republic, 2008.
47 P. Dumais, C. L. Callender, J. P. Noad and C. J. Ledderhof, *IEEE Sens. J.*, 2008, **8**, 457–464.
48 M. Kitsara, K. Misiakos, I. Raptis and E. Makarona, *Opt. Express*, 2010, **18**, 8193–8206.
49 J.-H. Kim, H.-Y. Yang and H.-Y. Lee, *Int. J. Mod. Phys. B*, 2009, **23**, 1891–1896.
50 A. Densmore, M. Vachon, D.-X. Xu, S. Janz, R. Ma, Y.-H. Li, G. Lopinski, A. Delage, J. Lapointe, C. C. Luebbert, Q. Y. Liu, P. Cheben and J. H. Schmid, *Opt. Lett.*, 2009, **34**, 3598–3600.
51 C. Hoffmann, K. Schmitt, A. Brandenburg and S. Hartmann, *Anal. Bioanal. Chem.*, 2007, **387**, 1921–1932.
52 K. Schmitt, B. Schirmer, C. Hoffmann, A. Brandenburg and P. Meyrueis, *Biosens. Bioelectron.*, 2007, **22**, 2591–2597.
53 A. Ymeti, J. Greve, P. V. Lambeck, T. Wink, S. W. F. M. van Hövell, T. A. M. Beumer, R. R. Wijn, R. G. Heideman, V. Subramaniam and J. S. Kanger, *Nano Lett.*, 2007, **7**, 394–397.
54 S. Pal, E. Guillermain, R. Sriram, B. Miller and P. M. Fauchet, *Frontiers in Pathogen Detection: From Nanosensors to Systems*, SPIE, San Francisco, CA, USA, 2010.
55 B. T. Cunningham and L. Laing, *Expert Rev. Proteomics*, 2006, **3**, 271–281.
56 M. R. Lee and P. M. Fauchet, *Opt. Lett.*, 2007, **32**, 3284–3286.

57 M. Lee and P. M. Fauchet, *Opt. Express*, 2007, **15**, 4530–4535.
58 S. Zlatanovic, L. W. Mirkarimi, M. M. Sigalas, M. A. Bynum, E. Chow, K. M. Robotti, G. W. Burr, S. Esener and A. Grot, *Sens. Actuators, B*, 2009, **141**, 13–19.
59 S. C. Buswell, V. A. Wright, J. M. Buriak, V. Van and S. Evoy, *Opt. Express*, 2008, **16**, 15949–15957.
60 D. Dorfner, T. Zabel, T. Hürlimann, N. Hauke, L. Frandsen, U. Rant, G. Abstreiter and J. Finley, *Biosens. Bioelectron.*, 2009, **24**, 3688–3692.
61 N. Skivesen, A. Têtu, M. Kristensen, J. Kjems, L. H. Frandsen and P. I. Borel, *Opt. Express*, 2007, **15**, 3169–3176.
62 S. Mandal and D. Erickson, *Opt. Express*, 2008, **16**, 1623–1631.
63 S. Mandal, J. M. Goddard and D. Erickson, *Lab Chip*, 2009, **9**, 2924–2932.
64 S. Arnold, M. Khoshsima, I. Teraoka, S. Holler and F. Vollmer, *Opt. Lett.*, 2003, **28**, 272–274.
65 A. M. Armani, R. P. Kulkarni, S. E. Fraser, R. C. Flagan and K. J. Vahala, *Science*, 2007, **317**, 783–787.
66 H. Zhu, I. M. White, J. D. Suter, P. S. Dale and X. Fan, *Opt. Express*, 2007, **15**, 9139–9146.
67 C. Y. Chao, W. Fung and L. J. Guo, *IEEE J. Sel. Top. Quantum Electron.*, 2006, **12**, 134–142.
68 A. Yalçin, K. C. Popat, J. C. Aldridge, T. A. Desai, J. Hryniewicz, N. Chbouki, B. E. Little, O. King, V. Van, S. Chu, D. Gill, M. Anthes-Washburn and M. S. Ünlü, *IEEE J. Sel. Top. Quantum Electron.*, 2006, **12**, 148–155.
69 A. Ramachandran, S. Wang, J. Clarke, S. J. Ja, D. Goad, L. Wald, E. M. Flood, E. Knobbe, J. V. Hryniewicz, S. T. Chu, D. Gill, W. Chen, O. King and B. E. Little, *Biosens. Bioelectron.*, 2008, **23**, 939–944.
70 C. A. Barrios, M. J. Bañuls, V. González-Pedro, K. B. Gylfason, B. Sánchez, A. Griol, A. Maquieira, H. Sohlström, M. Holgado and R. Casquel, *Opt. Lett.*, 2008, **33**, 708–710.
71 C. F. Carlborg, K. B. Gylfason, A. Kaźmierczak, F. Dortu, M. J. Bañuls Polo, A. M. Catala, G. M. Kresbach, H. Sohlström, T. Moh, L. Vivien, J. Popplewell, G. Ronan, C. A. Barrios, G. Stemme and W. van der Wijngaart, *Lab Chip*, 2010, **10**, 281–290.
72 K. M. De Vos, I. Bartolozzi, P. Bienstman, R. Baets and E. Schacht, *Nanoscale Imaging, Spectroscopy, Sensing, and Actuation for Biomedical Applications IV*, SPIE, San Jose, CA, USA, 2007.
73 A. L. Washburn, L. C. Gunn and R. C. Bailey, *Anal. Chem.*, 2009, **81**, 9499–9506.
74 K. De Vos, J. Girones, S. Popelka, E. Schacht, R. Baets and P. Bienstman, *Biosens. Bioelectron.*, 2009, **24**, 2528–2533.
75 P. Debackere, D. Taillaert, K. De Vos, S. Scheerlinck, P. Bienstman and R. Baets, *Silicon Photonics II*, SPIE, San Jose, CA, USA, 2007.
76 G.-D. Kim, G.-S. Son, H.-S. Lee, K.-D. Kim and S.-S. Lee, *Opt. Commun.*, 2008, **281**, 4644–4647.
77 M. Iqbal, M. A. Gleeson, B. Spaugh, F. Tybor, W. G. Gunn, M. Hochberg, T. Baehr-Jones, R. C. Bailey and L. C. Gunn, *IEEE J. Sel. Top. Quantum Electron.*, 2010, **16**, 654–661.
78 D.-X. Xu, A. Densmore, A. Delâge, P. Waldron, R. McKinnon, S. Janz, J. Lapointe, G. Lopinski, T. Mischki, E. Post, P. Cheben and J. H. Schmid, *Opt. Express*, 2008, **16**, 15137–15148.
79 X. Li, Z. Zhang, S. Qin, T. Wang, F. Liu, M. Qiu and Y. Su, *Appl. Opt.*, 2009, **48**, F90–F94.
80 M. Terrel, M. J. F. Digonnet and S. H. Fan, *Appl. Opt.*, 2009, **48**, 4874–4879.
81 H. Yi, D. S. Citrin, Y. Chen and Z. Zhou, *Appl. Phys. Lett.*, 2009, **95**, 191112–191113.
82 S. Wang, A. Ramachandran and S.-J. Ja, *Biosens. Bioelectron.*, 2009, **24**, 3061–3066.
83 M. S. Luchansky, A. L. Washburn, T. A. Martin, M. Iqbal, L. C. Gunn and R. C. Bailey, *Biosens. Bioelectron.*, in press, DOI: 10.1016/j.bios.2010.07.010.
84 M. S. Luchansky and R. C. Bailey, *Anal. Chem.*, 2010, **82**, 1975–1981.
85 A. L. Washburn, M. S. Luchansky, A. L. Bowman and R. C. Bailey, *Anal. Chem.*, 2010, **82**, 69–72.
86 A. J. Qavi and R. C. Bailey, *Angew. Chem., Int. Ed.*, 2010, **49**, 4608–4611.

